ACADÉMIE
DES SCIENCES
INSTITUT DE FRANCE

Comptes Rendus
Mécanique

Jean Varnier

Doppler effect considered as a distortion of time, application to an engineering case

Volume 353 (2025), p. 863-877

Online since: 18 July 2025

https://doi.org/10.5802/crmeca.312

The Comptes Rendus. Mécanique *are a member of the Mersenne Center for open scientific publishing*
www.centre-mersenne.org — e-ISSN : 1873-7234

ACADÉMIE DES SCIENCES
INSTITUT DE FRANCE

Comptes Rendus. Mécanique
2025, Vol. 353, p. 863-877
https://doi.org/10.5802/crmeca.312

Research article / *Article de recherche*

Doppler effect considered as a distortion of time, application to an engineering case

L'effet Doppler considéré comme une distorsion du temps, application à un cas d'ingénierie

Jean Varnier [a, b]

[a] French Aeronautical and Astronautical Association, 3AF, 75016 Paris, France

[b] National Office for Aerospace Studies and Research, ONERA, 92320 Châtillon, France

E-mail: varnierjean948@gmail.com

Abstract. The ground-based listening of aircraft, rockets, or space launchers, and the simulation of recorded acoustic spectra with a view to civilian or military applications, raise the problem of the distortion by the Doppler effect of the spectrum emitted by the sound sources, in addition to other problems related to the sound propagation in atmosphere. We propose a solution to the direct problem—the characteristics of the sound source and its trajectory are known—based on an original time approach to the Doppler effect. This study shows in fact that it is not necessary to distinguish between frequency and sound level variations, both being directly related to the ratio of the emission to the reception durations of a chosen signal sequence. The developed method has a character of generality and can be applied without restriction in most cases (e.g. variable speed of the mobile, curved trajectory, atmosphere with wind and temperature gradients) using an acoustic propagation code, but remains obviously applicable in an isotropic environment to simple or complex cases, for example when the observer is moving.

Résumé. L'écoute au sol d'avions, de fusées ou de lanceurs spatiaux, ainsi que la simulation de spectres acoustiques enregistrés en vue d'applications civiles ou militaires, soulèvent le problème de la distorsion par effet Doppler du spectre émis par les sources sonores, en plus d'autres problèmes liés à la propagation du son dans l'atmosphère. Nous proposons une solution au problème direct – les caractéristiques de la source sonore et sa trajectoire étant connues – basée sur une approche temporelle originale de l'effet Doppler. Cette étude montre en effet qu'il n'est pas nécessaire de distinguer les variations de fréquence et de niveau sonore, toutes deux étant directement liées au rapport des durées d'émission et de réception d'une séquence de signaux choisie. La méthode développée présente un caractère général et peut être appliquée sans restriction dans la plupart des cas (par exemple, vitesse variable du mobile, trajectoire courbe, atmosphère avec gradients de vent et de température) à l'aide d'un code de propagation acoustique, mais est évidemment applicable en environnement isotrope à des cas simples ou complexes, par exemple lorsque l'observateur est en mouvement.

Keywords. Aeroacoustics, Doppler effect, Time approach, Sound power spectrum, Sonic boom, Atmospheric propagation.

Mots-clés. Aéroacoustique, Effet Doppler, Approche temporelle, Spectre de puissance acoustique, Bang sonique, Propagation atmosphérique.

Manuscript received 25 May 2025, revised and accepted 30 June 2025.

1. Introduction

In the field of aeroacoustics, and more particularly in ground listening of aircraft or launch vehicles in flight, we are generally confronted with the following phenomena:

- the non-linearity of the sound source's trajectory;
- the variation of its speed over time;
- the anisotropic nature of the atmospheric propagation.

It is known, in particular, that the frequency spectrum emitted by the source is modified by the Doppler effect, and that the same is true for the sound level received at the listening point. The effects of atmospheric absorption also affect frequency and amplitude, but remain negligible at the frequencies of interest and at the distances and altitudes involved in the example discussed here.

In the 2000s, ONERA was led to address this issue as part of the Ariane 5 program of CNES and during studies on the noise environment of Military Aviation. It turned out that the classical geometric acoustics approach was not suited to the problem conditions, and that NASA's engineering approaches used complex and more or less empirical formalisms that were difficult to transpose to the experimental cases studied.

For these reasons, we were finally led to develop an original method, which was the subject of a first communication at the European Congress of Acoustics in 2008 [1], and which is developed here.

The purpose of this account is to describe this theoretical approach and the experimental case on which it was tested with a view to its validation.

2. State of art and aim of the study

The Doppler effect of moving acoustic sources, first discovered in 1842 by Christian Doppler, and more precisely developed in 1847 in the classical form of a frequency shift of a signal emitted by a moving harmonic sound source and perceived by a motionless observer [2], appears in various forms in many fields. From a theoretical point of view, the geometric approach to the Doppler effect is described for example in Ref. [3], the relativistic approach, valid in astronomical optics, in Ref. [4]. A time approach based on successive pulses emitted by the sound source is sometimes used, for educational purposes, to introduce the Doppler effect in the case where the source and the observer are located on the same axis [5]. In the continuation, our discussion concerns an application developed in an operational context in the domain of aeronautics.

In the field of aeroacoustics, the study of the Doppler effect is most often applied to the case of subsonic motion, the supersonic case generating certain particularities—duplication of the Doppler frequency already pointed out in [6], requiring some theoretical complements. In particular, it should be noted that despite a classical approach found in the literature for a long time [7,8], the harmonic sound sources and the Doppler effect are not responsible of the sonic boom, except in the purely theoretical case of a mobile reduced to a sound source of volume zero. In reality, it is the nose of the supersonic body which creates the shock front, so called Mach cone, responsible of the sonic boom, a phenomenon which is clearly not concerned by the Doppler effect [9].

In the 1960's, the literature mainly provided semi-empirical approaches applied to listening aircraft or rockets in flight, with a view to predict the spectrum and sound levels from jet noise received off the ground [10,11]. These models are generally accompanied by simplifying hypotheses (rectilinear trajectory, constant speed of the sound source, isotropic atmosphere) and applied to subsonic cases.

Otherwise, it is remarkable to note that while all publications agree on the calculation of frequencies shifted by the Doppler factor (see Section 3), there is a great disparity concerning the influence of the Doppler effect on sound levels. For example, in Ref. [12] we find a "convective amplification factor" where the Doppler factor is raised to the power 4, this exponent being reduced to 1.5 in another study [13]. Only [11] recommends, without further explanation, using the inverse of the Doppler factor to correct the sound level calculated at the reception point. As for the recent study [14], it takes into account spatial decrease of acoustic intensity, atmospheric attenuation and Doppler-shifted frequencies, but does not consider or address a Doppler correction of the calculated sound levels, which suggests either that it is forgotten or that it is assumed to be negligible compared to other parameters.

In fact, even in a fundamental work such as [3], the formula relating to the variation in sound level due to the Doppler effect is particularly complex and given without any explanation. It is also remarkable that no educational work on the Doppler effect, to our knowledge, mentions this question other than by attributing it to the variation in distance. Note that it is not easy to find studies in recent publications that include theoretical considerations on the Doppler effect.

In a first step, the objective of this study was to attempt to lighten the apparent disparities and uncertainties mentioned above and to free ourselves from the constraints that impose simplifying assumptions concerning the medium of sound propagation. In this perspective, we were led to imagine a time-domain approach that seems, at least from a theoretical point of view, simpler and more general than classical geometric approaches.

In particular, the speed of a sound source is likely to vary rapidly, its trajectory may be curved and not inscribed in a plane. The model must be able to calculate in frequency and amplitude the spectrum of the noise received at the listening point, apply indifferently to the subsonic case and the supersonic case, and be coupled with an acoustic propagation code in order to adapt to any atmospheric environment, standard, statistical or taken from a weather report.

3. Geometric approach

Considering the review above and the disparities we have encountered, we do not think it is useless to recall the physical and mathematical bases of the Doppler effect in aeroacoustics.

Figure 1 is a classic illustration of the Doppler effect in the subsonic case, considering a succession of spherical waves emitted at equal time intervals, i.e. the period of the harmonic or impulse source S moving at speed V, and opposite listening directions, where the perceived frequencies are continuously variable when the observer is not on the axis of the sound source's movement. The geometric representation of Figure 1 is convenient, because it allows to visualize the apparent modification of the wavelength of the signal according to a listening direction in relation to the sound source: either λ_1 in upstream direction (direct frequency, the source is getting closer), λ_2 in downstream direction (reverse frequency, the source is moving away).

Figure 2 pulled from [9] illustrates the supersonic case, where the Doppler effect only affects the sound sources within the acoustic zone, included in a "sound cone". The two propagation directions shown represent the doubling of Doppler frequencies: the one, emitted in forward direction, is called direct, the other, emitted in backward direction, is called reverse [6]. The two frequencies are perceived simultaneously by the same observer Δ when he is inside the sound cone. Both frequencies are confused and in theory become infinite on the sound cone (see Figure 3), also called Mach cone in the literature [2,7,8]. Knowing that the apparent wavelengths λ_1 and λ_2 become zero on this cone (Figure 4), a focus of the sound waves occurs, but in fact the sonic boom really heard corresponds to the shock fronts, so called N-wave, constituting the supersonic wake of Figure 2.

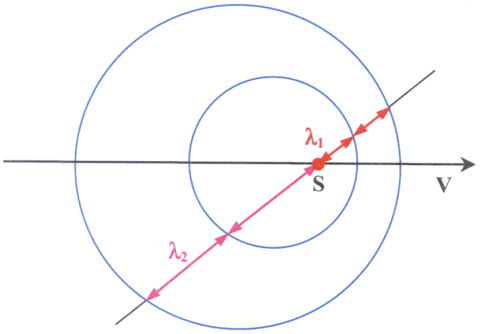

Figure 1. Subsonic case: apparent wavelengths in opposite listening directions.

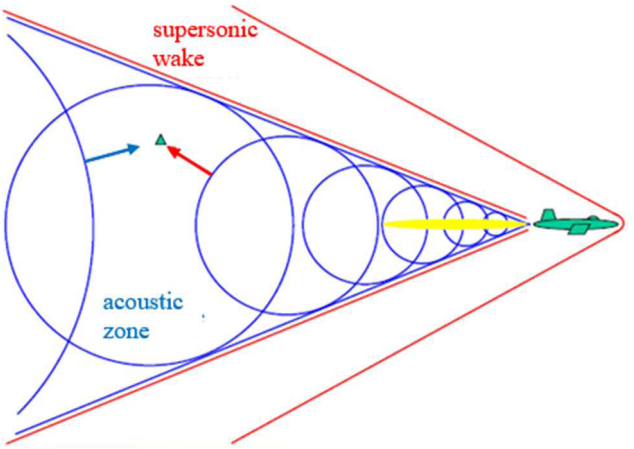

Figure 2. Supersonic case: shock wake and acoustic zone. Direct wave (blue arrow) and reverse wave (red arrow).

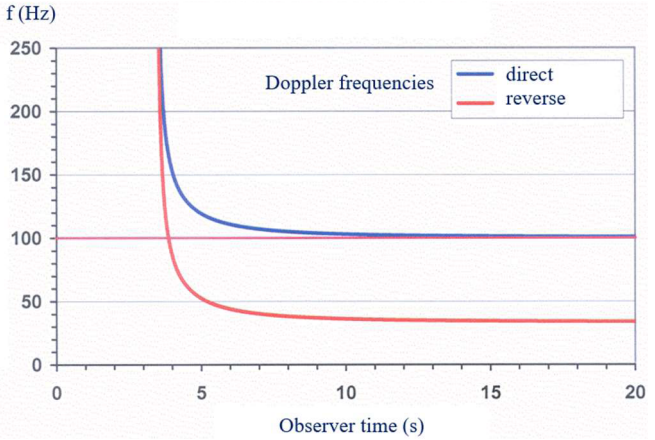

Figure 3. Doppler frequencies generated by a harmonic sound source of frequency 100 Hz moving at supersonic speed ($M = 2$).

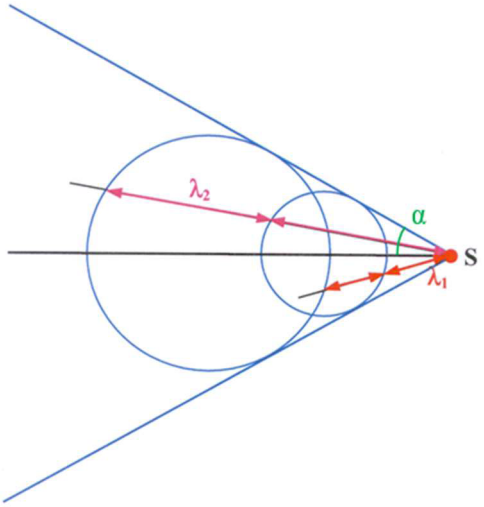

Figure 4. Supersonic case: sound cone, direct[1] and reverse[2] apparent wavelengths.

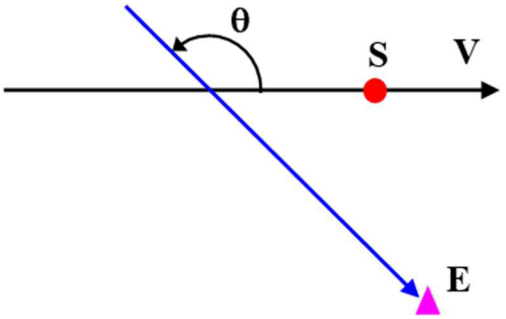

Figure 5. Direction of propagation θ for a listening point E linked to the fixed reference point.

Recall that the aperture α of the sound cone shown in Figure 4 is such that:

$$\sin\alpha = c/V = 1/M \tag{1}$$

where c is the speed of sound in the ambient medium and M is the Mach number.

The Doppler factor DF, which we define as the ratio of the frequency f perceived at the listening point linked to the fixed reference point and the frequency f_0 emitted by the moving sound source, is given by the classic formula:

$$\mathrm{DF} = f/f_0 = 1/(1 + M\cos\theta) \tag{2}$$

with the orientation conventions of Figure 5, the speed V of the source being subsonic or not. This formula is not much explicit but becomes evident, considering Figure 1, in the form:

$$\lambda_0/\lambda = c/(c + V\cos\theta) \tag{3}$$

where angle θ characterizes the listening direction with respect to the velocity vector V, see Figure 5 where the sound source S is represented at the moment when the wave considered reaches the listening point E.

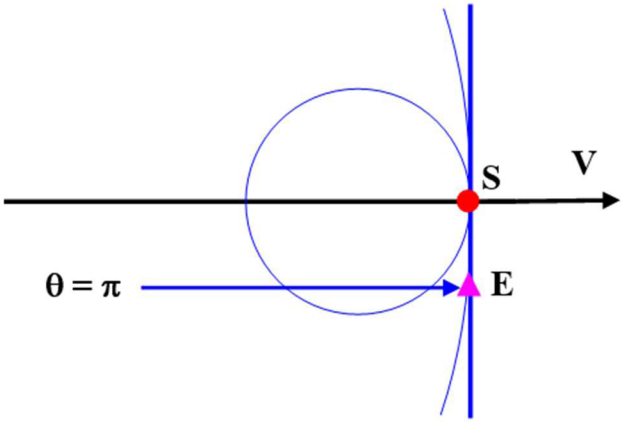

Figure 6. Sonic case: the sound waves emitted previously focus on a plane perpendicular to V passing through S.

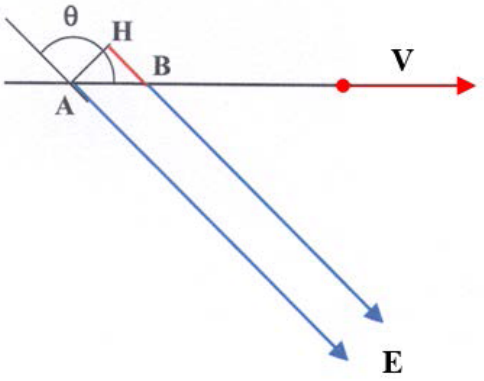

Figure 7. Case of a listening point E at infinity.

What happens when the velocity of the source tends towards the speed of sound? As shown in Figure 6, all the sound waves emitted forward in the preceding moments focus on a plane passing through S and perpendicular to the trajectory. This plane is equivalent to a sound cone whose half-angle at the apex α is $\pi/2$. The signal is perceived instantly at point E, in theory at any distance from the source: thus, everything happens as if the emission point was located upstream at infinity. We verify that formulas (2) and (3) give an infinite Doppler frequency f and a zero wavelength λ, the acoustic intensity also being infinite in theory.

4. Time approach

Figure 7 shows two acoustic beams emitted by source S at A at time t_A and at B at time t_B. The first beam reaches listening point E at time t_{E1}, the second at time t_{E2}.

Now suppose that E is far enough away so that the two beams are nearly parallel and that triangle AHB, where HB represents the path difference between the two beams, can be compared to a right triangle (note that the time interval $t_B - t_A$ can be chosen arbitrarily small).

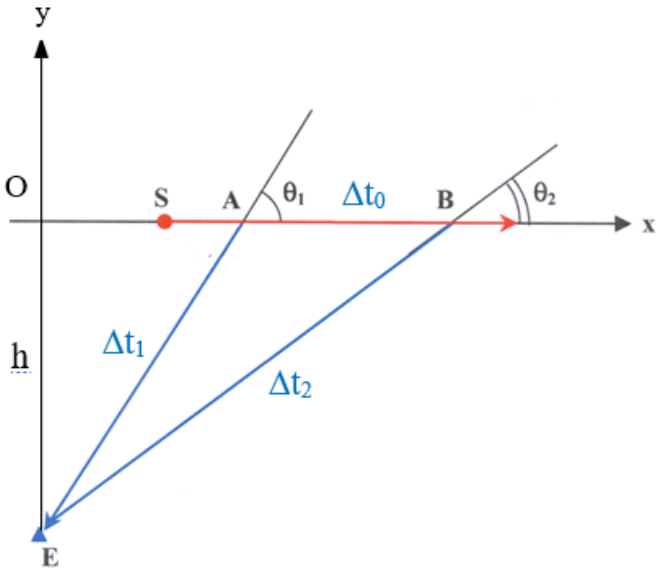

Figure 8. Case of a listening point E at a finite distance.

We can pose the following identities:

$$\begin{aligned} \mathrm{HB} &= -\mathrm{AB}\cos\theta \\ \mathrm{AB} &= Mc(t_\mathrm{B} - t_\mathrm{A}) \\ \mathrm{HB} + \mathrm{BE} &= \mathrm{AE} \\ \mathrm{AE} &= c(t_{\mathrm{E}1} - t_\mathrm{A}) \\ \mathrm{BE} &= c(t_{\mathrm{E}2} - t_\mathrm{B}). \end{aligned} \tag{4}$$

Substituting the values of the segments in the first equality, we obtain after simplification by c:

$$(t_\mathrm{B} - t_\mathrm{A})/(t_{\mathrm{E}2} - t_{\mathrm{E}1}) = 1/(1 + M\cos\theta) = \mathrm{DF}. \tag{5}$$

Thus the ratio of the time intervals at emission and reception, inverse of the frequency ratio, is equal to the Doppler factor DF and is identified with Equation (2). This calculation can therefore be considered as a demonstration of the general formula from a virtual displacement of the emission point.

We can notice that the first two equalities of (4) allow us to write the geometric relation:

$$\cos\theta = (\mathrm{BE} - \mathrm{AE})/\mathrm{AB} \tag{6}$$

We now consider the case where the observation point is at a finite distance from the trajectory of the source (Figure 8). The atmosphere is assumed to be homogeneous (c is constant), the trajectory rectilinear and the speed V of the source S constant. The harmonic source emits spherical waves of which two rays passing through the listening point E are indicated.

Let Δt_0 be the time taken by S to travel to AB, Δt_1 the propagation time between A and E, Δt_2 the propagation time between B and E. The rays therefore arrive at E at times Δt_1 on the one hand, and $\Delta t_0 + \Delta t_2$ on the other hand. The ratio between the reception time $(\Delta t_0 + \Delta t_2) - \Delta t_1$ and the emission time Δt_0 is therefore equal to:

$$1 + (\Delta t_2 - \Delta t_1)/\Delta t_0 = 1/\langle \mathrm{DF} \rangle \tag{7}$$

In light of Equation (5), we postulate that this ratio is equal to the inverse of the average value, noted $\langle \mathrm{DF} \rangle$, of the Doppler factor at the listening point when the source travels the distance AB.

The trigonometric relationships in triangle ABE allow us to write:

$$\mathrm{AB}/\sin(\theta_1-\theta_2) = \mathrm{AE}/\sin\theta_2 = \mathrm{BE}/\sin\theta_1 \tag{8}$$

knowing that:

$$\begin{aligned} \mathrm{AB} &= V\Delta t_0 = Mc\Delta t_0 \\ \mathrm{AE} &= c\Delta t_1 \\ \mathrm{BE} &= c\Delta t_2 \end{aligned} \tag{9}$$

Equation (8) can be written:

$$M\Delta t_0/\sin(\theta_1-\theta_2) = \Delta t_1/\sin\theta_2 = \Delta t_2/\sin\theta_1 \tag{10}$$

We can deduce from Equation (8) the geometric identity:

$$(\mathrm{BE}-\mathrm{AE})/\mathrm{AB} = (\sin\theta_1-\sin\theta_2)/\sin(\theta_1-\theta_2) \tag{11}$$

and from Equations (7) and (10) the identity:

$$1/\langle \mathrm{DF}\rangle = 1 + [(\sin\theta_1-\sin\theta_2)/\sin(\theta_1-\theta_2)]M \tag{12}$$

By analogy with Equations (2) and (6), we can assume that the expression in brackets is equal to the average value of $\cos\theta$ between points A and B, which according to (11) can be written in two different ways:

$$\langle\cos\theta\rangle = (\mathrm{BE}-\mathrm{AE})/\mathrm{AB} = (\sin\theta_1-\sin\theta_2)/\sin(\theta_1-\theta_2) \tag{13}$$

The sine in the denominator, unusual in the expression of the average value of a cosine, corresponds to the fact that the variation of the angle θ is not linear along the segment AB.

Since Equation (8) is true for all values of the angles θ_1 and θ_2, we can verify Equation (11) by arbitrarily fixing one of the two angles. It is convenient to choose $\theta_1 = \pi/2$ which corresponds to the origin O of the coordinate system in Figure 6. For simplicity, we also set $\theta_2 = \theta$. If x is the abscissa of the current point on the trajectory and h the ordinate of the listening point E, we immediately have:

$$\cos\theta = x/\sqrt{(x^2+h^2)} \tag{14}$$

The average value of the cosine over the interval Ox is then obtained by integration as a function of the variable x and division by x, the value $-h$ of the integration constant being given by the initial conditions $\theta = \pi/2$ and $x = 0$. We arrive at:

$$\langle\cos\theta\rangle = \sqrt{(1+h^2/x^2)} - h/x \tag{15}$$

expression which tends towards 0 when x tends towards 0. Noting that $h/x = \tan\theta$, we can still write:

$$\langle\cos\theta\rangle = 1/\cos\theta - \tan\theta \tag{16}$$

We verify that this is also the form that Equation (9) takes when we set $\theta_1 = \pi/2$ and $\theta_2 = \theta$, which demonstrates the proposition. As expected, we can write Equation (12) in the form:

$$1/\langle \mathrm{DF}\rangle = 1 + M\langle\cos\theta\rangle \tag{17}$$

expression that extends Equation (2) to an interval of any duration. Equation (13) also gives:

$$\langle\cos\theta\rangle = (\mathrm{BE}-\mathrm{AE})/\mathrm{AB} \tag{18}$$

relationship which has the practical interest of calculating the average cosine on a scale drawing. If we assume a real configuration where the angles of Figure 6 are respected and where a sound source emitting a dominant frequency of 100 Hz passes from points A to B at a speed of Mach 0.2, we obtain by simple measurement of the lengths of Figure 6: $\langle\cos\theta\rangle \approx 0.69$, $\langle \mathrm{DF}\rangle \approx 0.88$, and the frequency perceived at E, $\langle f\rangle \approx 88$ Hz.

5. Generalization

To summarize the previous paragraph, we can say that in the classical configuration where the trajectory is rectilinear, the speed of the source constant and the propagation medium isotropic, the average Doppler factor between two points of the trajectory and for a given observation point is equal to:

$$\langle \mathrm{DF} \rangle = \Delta t_\mathrm{S} / \Delta t_\mathrm{R} \tag{19}$$

where Δt_S denotes the duration of the signal at emission and Δt_R the duration of the signal at reception. This duration Δt_R depending of many factors, the relationship (19) leads us to considering the Doppler effect as a distortion of the time between the emission and the reception—distortion meaning in physics "lack of proportionality between the signal emitted and the signal received". This phenomenon obviously causes a shift in frequency as well as a variation in acoustic intensity, by assuming that the acoustic energy is conserved, apart from absorption phenomena, in a given emission volume.

This being admitted, we see that Equation (12) is indifferent to the phenomena that can occur between transmission and reception, at least to the refraction of sound rays by the wind and to temperature gradients, and that the same is true for the phenomena that determine the transmission: trajectory, speed and acceleration of the sound source, variation of its power over time. However, the calculation will only be of interest if we consider a time step sufficiently short compared to the scale of the variations of these parameters. The frequencies f_R and the levels L_R of acoustic intensity calculated at the reception point without taking, in a first step, the Doppler effect into account, will be modified as follows by the Doppler factor to give the final values:

$$f_\mathrm{D} = f_\mathrm{R}(\Delta t_\mathrm{S} / \Delta t_\mathrm{R}) \tag{20}$$

$$L_\mathrm{D} = L_\mathrm{R} + 10 \log(\Delta t_\mathrm{S} / \Delta t_\mathrm{R}) \tag{21}$$

Thus, frequency and acoustic intensity are governed by the same ratio equal to the Doppler factor. This relationship, which seems us fundamental, is neither used nor pointed out in the literature we consulted, except in Ref. [11] which indicates for supersonic jets a shift in sound power level of $10 \log 1/\mathrm{DF}$ instead $10 \log \mathrm{DF}$ (page 17), unless there is an error in the sign.

Figures 9 and 10 summarize the issues to be considered in real-world situations. Figure 9 does not show the wind direction at successive altitudes, which generally needs to be considered. In this case, the ray paths shown in Figure 10 would probably not be included in a plane. The process consists of choosing a time step $\Delta t_\mathrm{S} = t_2 - t_1$ along the sound source trajectory, and of calculating, using a sound ray computer code, the corresponding signal duration $\Delta t_\mathrm{R} = t'_2 - t'_1$ at the listening point E. Equations (20) and (21) then give the correction to be applied to the frequencies and sound levels f_R and L_R obtained in static mode, in order to compare with the experimental data the final results f_D and L_D integrating the Doppler effect.

6. Application case

We see that the approach described above allows us to calculate the Doppler effect from signal durations, beyond any other considerations, provided we are able to calculate, when they exist, the trajectories of the acoustic rays that leave each chosen calculation point and pass through the reception point, as well as their propagation times. This requires knowing the trajectory of the sound source, the characteristics of the acoustic emission and the atmospheric conditions, as well as taking into account atmospheric absorption and Earth's roundness when the distance requires it. This problem and its converse, consisting of calculating the trajectories of fictitious rays coming from the listening point to target the acoustic source, were addressed at ONERA as part of a study conducted in another context [15].

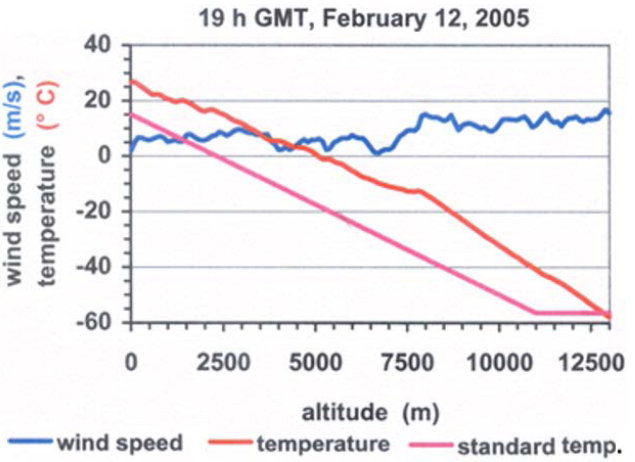

Figure 9. Example of a real atmosphere compared to a standard atmosphere without wind.

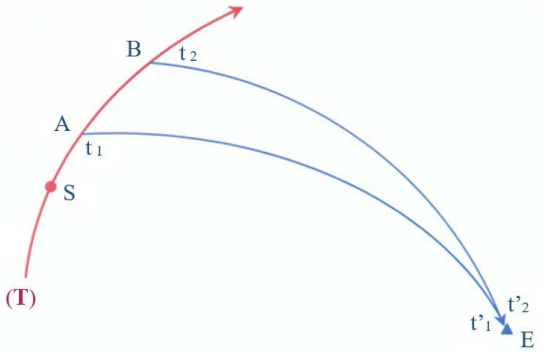

Figure 10. General case of any sound source trajectory and non-straight sound ray trajectories.

This model concerning the Doppler effect was developed in the framework of the Ariane 5 program of the French National Center for Space Studies (CNES). It involved to test in a dynamic context the jet noise model developed by the ONERA, based on NASA studies and improved from static firings of rocket engines of different sizes, up to a ballistic missile first stage [16]. More precisely, the proposed objective was to reproduce the "acoustic fallout" recorded in Kourou by the "Toucan" listening station of ONERA, 4800 m from the launch pad, during the initial phase of Flight 521 of the Ariane 5 space launcher.

In such a take-off context, the problem arises of the orientation of the launcher speed in the opposite direction to that of the jets and therefore of the noise sources emitted downstream at an initially supersonic speed. Since no classical model seems to be able to adapt to this particular configuration, we finally imagined the time approach described previously and formulated the following hypothesis: the jets being included in the aerodynamic wake and quickly protected by the supersonic shock wake of the launcher (see Figure 2), their emitted noise spectrum must remain fairly close to that of static firings and there is no need, in a first analysis, to modify the jet noise model used. Such a hypothesis is also adopted in Ref. [11] for supersonic jets, but a "convection Mach number" where the vehicle speed is subtracted from jet speed is used in the subsonic case.

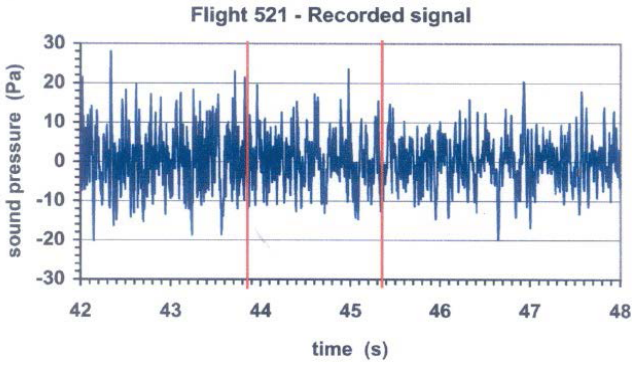

Figure 11. Signal recorded by the "Toucan" station. Launcher altitude 3100 to 4600 m, signal analysis window centered at 3750 m.

This being established, it remained to use the data provided by the CNES, namely the position as a function of time of the launcher and therefore of the acoustic emission zone, which makes it possible to calculate the propagation times of the sound rays towards the listening station and to determine the value of the Doppler factor in successive time intervals. The length of the sound rays also gives the spatial decrease in the acoustic level for the portion of the trajectory considered, and their direction relative to the axis of the jets makes it possible to calculate the acoustic power spectrum to be taken into account. Since no sonic boom is perceived, it is concluded that the listening station remains inside the sound cone and receives only the "reverse" Doppler frequencies (see Section 2 and Figure 2).

The particularly favorable atmospheric conditions (see Figure 9) made it possible to use a simplified propagation model mainly taking into account a temperature gradient very close to that of the standard atmosphere [J], the influence of the wind being considered as negligible. In addition to the uncertainties linked to the simulation of the acoustic emission and to the aerodynamic disturbances in flight, the position of the free-field microphones at height (about 2.5 m over a low vegetation) raised the question of the reflected sound field, which led us to compare the measurements with the sound levels calculated in free field on the one hand, above a fictitious reflective plane on the other hand (sound level increased by 3 dB). Note that the trajectory of the launcher is not straight, it bends rapidly in an easterly direction.

We present two calculations corresponding to a case where the launcher speed is subsonic, below an altitude of 4000 m, and to a case where it is supersonic, around an altitude of 13,000 m. Figures 11 and 12 give the acoustic pressures recorded by station "Toucan" in each case at the acquisition frequency of 5 kHz, and in red the calculated arrival times of two sound rays emitted in altitude at one second interval: this allows a direct reading of the value of the average Doppler factor of the framed period, i.e. $\langle \mathrm{DF} \rangle = 1\ \mathrm{s}/1.5\ \mathrm{s} = 0.667$ in the first case, $\langle \mathrm{DF} \rangle = 1\ \mathrm{s}/2.6\ \mathrm{s} = 0.385$ in the second. This allows us to calculate the "apparent speed" of the launcher using formula (2), knowing that the angles of the sound rays with the trajectory are $\theta \approx 50°$ and $\theta \approx 22°$ respectively: we obtain $M \approx 0.78$ in the first case, $M \approx 1.72$ in the second.

Figures 13 and 14 give on the one hand the sound power spectral density from the signals of Figures 11 and 12 between the red time markers (dark blue curve), on the other hand the raw result of the simulation of the jet noise from the three rocket engines of the launcher at a distance equal to the length of the calculated sound rays (sky blue curve), finally the framing obtained by integrating the Doppler factor by means of Equations (20) and (21), in the presence or not of a reflected field (purple and red curves).

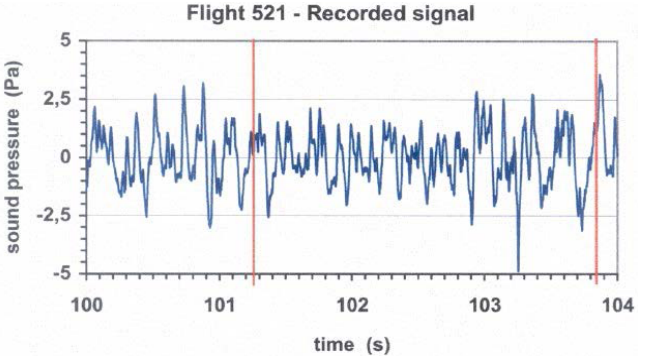

Figure 12. Signal recorded by the "Toucan" station. Launcher altitude 11,700 to 13,700 m, signal analysis window centered at 13,000 m.

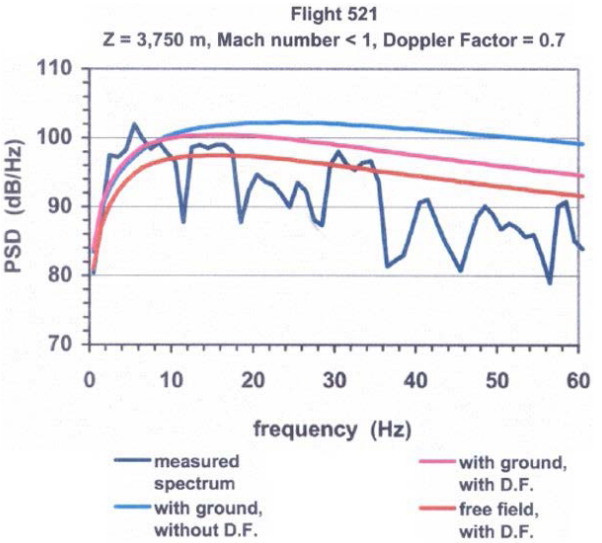

Figure 13. Sound power spectral density for the window in Figure 11. Simulations without and with Doppler factor.

Knowing that the jet noise spectrum is very regular in the case of static firings of small rocket engines (boosters at scales 1/20 and 1/10), it appears that the measured noise spectrum in Figure 13, which corresponds to the signal between the two time marks in Figure 11, seems to be strongly disturbed by the aerodynamic effects due to the vortex wake of the launcher at subsonic speed, but that the envelope of the maxima given by the model nevertheless appears to be correct.

In Figure 14, the noise spectrum corresponding to the period indicated in Figure 12 has the same general appearance but is much more regular, the jets being apparently shielded by the shock wake of the launcher at supersonic speed. The slope of the spectrum is clearly accentuated compared to that of Figure 13, because of the decreasing value of the Doppler factor. It can be said that the "free field" simulation (red curve) is very satisfactory up to 50 Hz, the drop in the measured noise level below 3 Hz being probably due to the cut-off frequency of the measurement devices. In contrast, the minima at 28 and 36 Hz, visible in both figures, probably have a physical cause.

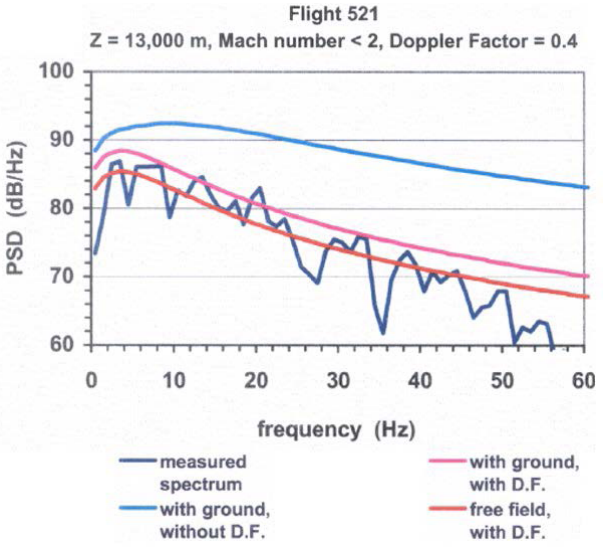

Figure 14. Sound power spectral density for the window in Figure 12. Simulations without and with Doppler factor.

We can admit that the results of the simulations constitute an apparent validation of the models used and of the simplifying assumptions that accompanied their implementation. It appears in particular that the diminution of sound levels by the Doppler effect (−2 dB in case of Figure 13, −4 dB in case of Figure 14), sometimes omitted in previous or contemporary studies, has improved the accuracy of the calculation.

7. Conclusion

Despite the uncertainties mentioned, the application example given in Section 6 can be considered as a first validation by experience of the method of calculating the Doppler effect applied to aerial sound sources stemming from a supersonic vehicle. More generally, the specificity of the model is that it can be applied to any trajectory and to a real environment, unlike geometric models whose field of application is restricted by the assumptions of the rectilinear and uniform displacement of the sound source, and above all of a homogeneous and isotropic propagation medium.

The approach described, which proposes calculating the Doppler factor from the duration of the emitted and received signals, is equivalent to attributing the cause to a distortion of time, distortion being understood in the physical sense of a lack of proportionality between the emitted and received signals.

It should be noted that the principle of conservation of acoustic energy in a given emission volume, omitting the atmospheric absorption effects, allows to apply the Doppler factor to both acoustic intensity and frequency. In our opinion, this assertion represents a step forward in the understanding of these phenomena, given that the variation of sound levels due to the Doppler effect does not have a well-defined formulation in the literature: its calculation is in fact either clearly empiricist without obvious theoretical justification, or simply omitted.

The model applies to sound sources linked up to both subsonic and supersonic vehicles. In the latter case, regarding the Doppler effect, the definition of the Mach cone created by a point harmonic source, and upon passage of which a sonic boom is perceived, is often found in

the literature. This may be true theoretically, but it should be noted that the sonic boom caused by the passage of a supersonic aircraft is only related to the shock wake created in the atmosphere by the body of the mobile, and is therefore neither caused nor modified by the Doppler effect. We felt it was important to clarify this point.

The major difficulty relating to the model, apart from the classical cases in homogeneous and isotropic medium where it applies directly, is that it must be coupled with an acoustic propagation computer code to calculate, by integrating the wind and temperature data, the path of the sound rays and their travel time between the emission points chosen and the listening point. The main difficulty consists in correctly targeting the listening point, so as to minimize the number of iterative calculations. This problem has been solved at the ONERA, in particular by making reversible the calculation of the sound rays, which was theoretically impossible in the presence of wind gradients, due to the inversion of the concavity of the ray trajectories [17]: as it is proposed in Ref. [15], to make it possible it was in fact sufficient to reverse, at all altitudes, the direction of the wind given by the weather report.

Declaration of interests

The author does not work for, advise, own shares in, or receive funds from any organization that could benefit from this article, and has declared no affiliations other than his research institution.

Acknowledgements

The author expresses his gratitude to Geraldine Ménexiadis, PhD, Claude Bresson, Research Engineer, and Georges Elias, PhD, Research Director at the National Office for Aerospace Studies and Research (ONERA).

References

[1] J. Varnier, "Doppler effect in aeroacoustics", *J. Acoust. Soc. Am.* **123** (2008), no. 5, p. 3248.
[2] D. D. Nolte, "The fall and rise of the Doppler effect", *Phys. Today* **73** (2020), no. 3, pp. 30–35.
[3] P. M. Morse and K. U. Ingard, *Theoretical Acoustics*, Sound Emission from Moving Sound Sources, McGraw-Hill Book Co.: New York, 1968, pp. 717–736.
[4] T. P. Gill, *The Doppler Effect - An Introduction to the Theory of the Effect*, Logos Press Ltd., Academic Press Inc.: London, 1965.
[5] J. Lamirand and M. Joyal, *Physique*, Mathématiques & Sciences Expérimentales, Masson et Cie: Paris, 1964.
[6] E. Esclangon and P. Charbonnier, *L'acoustique des canons et des projectiles. Etude cinématique du champ acoustique d'un projectile*, Mémorial de l'Artillerie Française, vol. 4, Imprimerie Nationale, Editions Gauthier-Villars et Cie: Paris, 1925. 3$^{\text{éme}}$ fascicule.
[7] F. Coulouvrat, "Le bang sonique", *Pour la Sci.* (2001), pp. 24–29. Special Issue "Le Monde des Sons".
[8] T. Walsh, "The Doppler effect and sonic boom", in *Physics: Interactive Physics Simulations, Waves, Circa*, 2020. Online at https://ophysics.com/waves11.html (accessed on April 30, 2025).
[9] J. Varnier, "Sonic boom, jet noise and Doppler effect", *Acoust. Pract. EAA* **1** (2013), no. 2, pp. 7–15.
[10] G. A. Wilhold, S. H. Guest and J. H. Jones, *A technique for predicting far-field acoustic environments due to a moving rocket sound source*, NASA Technical Note D-1832, Stanford University Libraries, Hathi Trust, 1963. ISSN 0499-9339.
[11] J. R. Stone, *Interim prediction method for jet noise*, NASA Technical Memorandum, NASA TM X-71618, NASA Technical Reports Server NTRS, 1974.
[12] R. H. Burrin, K. K. Ahuja and M. Salikuddin, "High speed flight effects on noise propagation", in *AIAA-87-0013, 25th AIAA Aerospace Sciences Meeting, Reno, NV, USA, 24–26 March 1987*, AIAA Research Central, arc.aiaa.org, 1987.
[13] P. Drevet, J. P. Duponchel and J. R. Jacques, "The effect of flight on jet noise as observed on the Bertin Aérotrain", *J. Sound Vib.* **54** (1977), no. 2, pp. 173–201.

[14] M. Snellen, R. Merio-Martinez and D. G. Simons, "Assessment of noise variability of landing aircraft using phased microphone array", *J. Aircr.* **54** (2017), no. 6, pp. 2173–2183.

[15] G. Ménéxiadis and J. Varnier, "Long-range propagation of sonic boom from the Concorde airliner: analyses and simulations", *J. Aircr.* **45** (2008), no. 5, pp. 1612–1618.

[16] J. Varnier, "Experimental study and simulation of rocket engine free jet noise", *AIAA J.* **39** (2001), no. 10, pp. 1851–1859.

[17] J. Vermorel, *Extension du principe de Fermat à un milieu en mouvement*, Technical Report, French-German Research Institute of Saint-Louis ISL, 1987.